

# EXPLORING AMYLOID-ASSOCIATED CEREBRAL VASCULOPATHY IN AN AGED NONHUMAN PRIMATE MODEL BY MULTIPARAMETRIC MRI

Silun Wang<sup>1</sup>, Jeromy Dooyema<sup>2</sup>, Xiaodong Zhang<sup>1</sup>, Lary C. Walker<sup>2,3</sup>, and Eric Heuer<sup>2,4</sup>

<sup>1</sup>Yerkes Imaging Center, Yerkes National Primate Research Center, Emory University, Atlanta, GA, United States, <sup>2</sup>Yerkes National Primate Research Center, Emory University, GA, United States, <sup>3</sup>Department of Neurology, Emory University, GA, United States, <sup>4</sup>University of Hawaii at Hilo, HI, United States

**Target audience:** MRI scientists, radiologists, neurologists and pathologists.

**Purpose:** Cerebral  $\beta$ -amyloid angiopathy (CAA) commonly occurs in patients with Alzheimer's disease, especially in patients with the apolipoprotein E (APOE)  $\epsilon 4$  genotype<sup>1</sup>. CAA has been linked to increased hemorrhage, inflammation, and leukoaraiosis, but definitively identifying these sequelae of CAA in the living brain is difficult<sup>1</sup>. Quantitative analysis of diffusion tensor imaging (DTI) indices has shown promise in the evaluation of neuropathological changes such as astrogliosis, demyelination, and axonal injury in pre-clinical animal models<sup>2,3</sup>. Susceptibility-Weighted Imaging (SWI) enhances the detection of iron-rich structures, thus providing highly sensitive and specific detection of cerebral microbleeds. However, because of the long time that usually elapses between scanning and histopathologic analysis, virtually nothing is known about how SWI and DTI indices are related to specific and concurrent pathological changes associated with CAA. In a nonhuman primate model of CAA<sup>4</sup>, we employed multiparametric MRI to link anomalies detected *ex vivo* to specific histopathologic changes in aged squirrel monkeys.

**Methods:** *Animal model preparation:* Under deep pentobarbital anesthesia, the brains of 6 squirrel monkeys were perfusion-fixed with 4% phosphate-buffered paraformaldehyde. The brains then were embedded in 2% agar phantoms for *ex vivo* imaging in a 7T MR scanner (Bruker, Germany) with a quadrature surface coil.

**MRI scanning:** Whole brain T2-Weighted imaging (T2WI), SWI and DTI were performed using the following imaging parameters: T2WI: TR/TE=1000ms/50ms, FOV = 4.0 mm<sup>2</sup>, thickness= 1mm, acquisition matrix = 128 x 128. The SWI measurements used a 3-dimensional FLASH sequence that is very sensitive to the presence of paramagnetic substances such as iron-compounds. The 3D FLASH sequence was performed using a voxel resolution of 0.078  $\times$  0.078  $\times$  0.156 mm<sup>3</sup>, 3D matrix=256 x 256 x 128, TE/TR=5ms/60ms, FOV=45mm x 45mm, NEX=8. DTI was acquired using multiple-slice, spin echo sequences with TR/TE = 7500ms/35ms, FOV = 45mm x 45 mm, thickness= 1mm, data matrix = 128 x 128, in-plane resolution = 0.35  $\times$  0.35 mm<sup>2</sup>. 30 gradient directions were employed with b value =0, 1000 s/mm<sup>2</sup>, respectively. **Imaging procession:** FA,  $\lambda_{ff}$  and  $\lambda_L$  diffusivity maps were derived for quantitative analysis using DTIstudio v2.4 (Johns Hopkins University). DTI indices were analyzed by ROIs drawn over occipital white matter tracts and gray matter using Image J (NIH, U.S) (Fig 1). Paired *t*-test was used to detect statistical differences in DTI indices between diseased/control gray matter and white matter. The SWI images were generated with a filter full-width of 128 and a phase mask multiplication of 4 during the image data collection. The in-house software SPIN was used for image processing. **Histological evaluations:** After MR imaging, histological sections through regions of interest were cut on a sliding microtome and immunostained for  $\beta$ -amyloid (antibody 6E10), microglia (antibody to IBA1), astrocytes (antibody to GFAP), myelin (antibody to myelin basic protein), and with Perls' stain (for iron deposition) or hematoxylin and eosin.

**Results:** *SWI detection of abnormalities in gray matter:* SWI clearly identified areas of hypointensity in several aged monkeys. In one animal in particular, a region in the occipital lobe showed a large hypointense region that was shown by histology to contain abnormal iron deposits as well as astrogliosis, microgliosis and advanced CAA (Figure 1 and 2). Myelin basic protein intensity appeared normal in the adjacent white matter. **DTI indices in diseased white matter and gray matter:**

The only significant difference was detected between the diseased/control groups was found in the gray matter, where the ADC values were significantly higher in controls than in the diseased group ( $0.65 \pm 0.12$  vs.  $0.88 \pm 0.10 \times 10^{-3}$  mm<sup>2</sup>/s,  $p < 0.05$ ). No significant differences in other DTI indices were observed in other regions.

**Conclusion:** (1) SWI imaging provides useful diagnostic information for CAA-related changes in the aged brain. (2) Significantly decreased ADC values may reflect multiple pathological changes, including microgliosis, astrogliosis and  $\beta$ -amyloid deposition in the walls of cerebral blood vessels. (3) Our results support the use of SWI and DTI as noninvasive imaging modalities to explore microvascular changes in nonhuman primate models. (4) This model could be employed to elucidate the mechanisms of neurodegenerative disease and to monitor treatment response *in vivo*.

**References :** 1. Poel et al., Stroke, 2010; 41 :S103-6; 2. Jiang et al, Neuroimage, 2006;32:1080-1089; 3. Wang et al., Cancer research 2009;69:1190-7; 4. Heuer et al., Curr Pharm Des., 2012;18:1159-1169; 5. Wang et al., Stroke 2008; 39: 2348-2353.

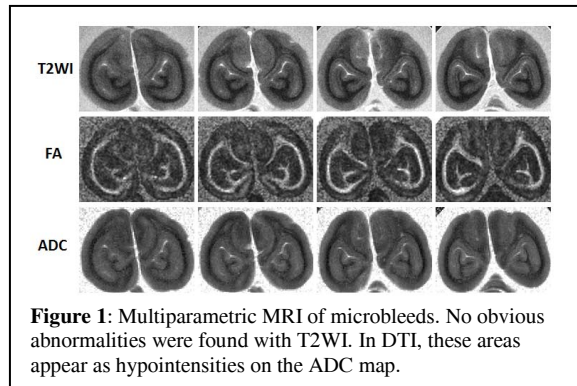


**Figure 1:** Multiparametric MRI of microbleeds. No obvious abnormalities were found with T2WI. In DTI, these areas appear as hypointensities on the ADC map.

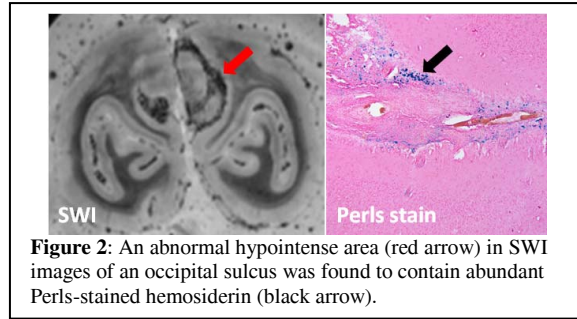


**Figure 2:** An abnormal hypointense area (red arrow) in SWI images of an occipital sulcus was found to contain abundant Perls-stained hemosiderin (black arrow).

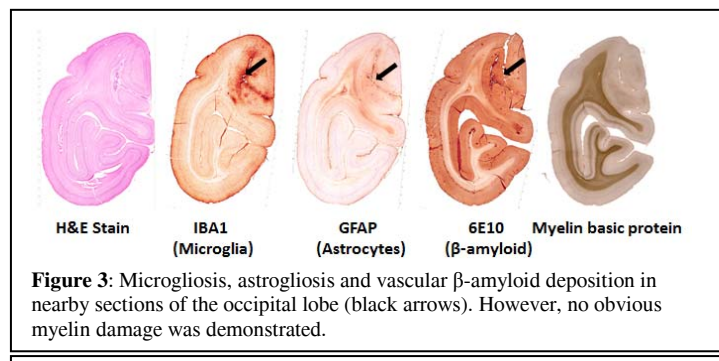


**Figure 3:** Microgliosis, astrogliosis and vascular  $\beta$ -amyloid deposition in nearby sections of the occipital lobe (black arrows). However, no obvious myelin damage was demonstrated.

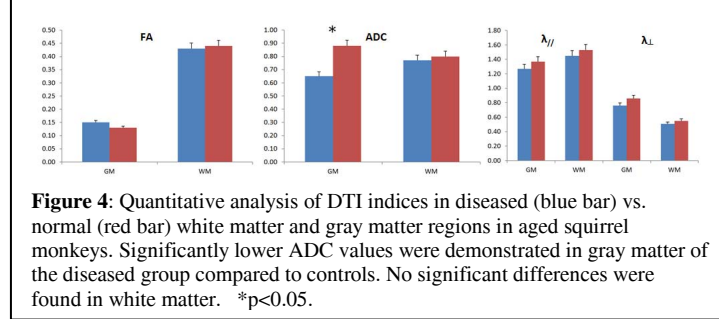


**Figure 4:** Quantitative analysis of DTI indices in diseased (blue bar) vs. normal (red bar) white matter and gray matter regions in aged squirrel monkeys. Significantly lower ADC values were demonstrated in gray matter of the diseased group compared to controls. No significant differences were found in white matter. \* $p < 0.05$ .